UHD-IQA Benchmark Database: Pushing the Boundaries of Blind Photo Quality Assessment

Vlad Hosu[1], Lorenzo Agnolucci[1,3], Oliver Wiedemann[2], and Daisuke Iso[1]

[1] Sony AI – [name.surname@sony.com]
[2] University of Konstanz, Germany – [name.surname@uni-konstanz.de]
[3] University of Florence, Italy – [name.surname@unifi.it]

Abstract. We introduce a novel Image Quality Assessment (IQA) dataset comprising 6073 UHD-1 (4K) images, annotated at a fixed width of 3840 pixels. Contrary to existing No-Reference (NR) IQA datasets, ours focuses on highly aesthetic photos of high technical quality, filling a gap in the literature. The images, carefully curated to exclude synthetic content, are sufficiently diverse to train general NR-IQA models. Importantly, the dataset is annotated with perceptual quality ratings obtained through a crowdsourcing study. Ten expert raters, comprising photographers and graphics artists, assessed each image at least twice in multiple sessions spanning several days, resulting in highly reliable labels. Annotators were rigorously selected based on several metrics, including self-consistency, to ensure their reliability. The dataset includes rich metadata with user and machine-generated tags from over 5,000 categories and popularity indicators such as favorites, likes, downloads, and views. With its unique characteristics, such as its focus on high-quality images, reliable crowdsourced annotations, and high annotation resolution, our dataset opens up new opportunities for advancing perceptual image quality assessment research and developing practical NR-IQA models that apply to modern photos. Our dataset is available at https://database.mmsp-kn.de/uhd-iqa-benchmark-database.html.

Keywords: NR-IQA · Dataset · UHD

1 Introduction

1.1 Motivation

No-Reference Image Quality Assessment (NR-IQA) can revolutionize various applications by automatically evaluating perceptual image quality without requiring a reference. However, NR-IQA models must accurately predict quality and generalize robustly across diverse distortions to realize this potential. Current NR-IQA methods perform well on images with pronounced distortions at Standard Definition (SD) resolutions but struggle on higher-resolution images with subtle quality degradations [6, 23]. Modern cameras commonly capture UHD+

Fig. 1: Sample images from our dataset. The authors of the images are, from left to right, top to bottom: 'Bergadder', 'Daria-Yakovleva', 'Quangpraha', 'StockSnap', 'pcdazero', and 'Free-Photos' from Pixabay.com.

images, on which existing NR-IQA models are inaccurate and inefficient. Moreover, no IQA datasets specifically target the high-quality range at high resolutions (HR-HQ), which is crucial for discerning subtle degradation. Such fine-grained quality assessment is essential for camera benchmarking, professional-grade photo curation, and optimizing camera parameters. Therefore, to unlock the full potential of NR-IQA, we need novel datasets and models that reliably subjectively assess high-resolution images across the high-quality spectrum.

1.2 Problem and challenges

Only a small fraction of existing IQA datasets are annotated at high resolutions. This is insufficient for training models that generalize well to high resolutions. Furthermore, current datasets are heavily skewed towards average-quality images, with below 1% having excellent quality, i.e., mean opinion scores (MOS) exceeding 90% of the quality scale. This severe under-representation of high-quality images is a typical example of a class imbalance problem, which impairs model performance. High-resolution IQA datasets are needed to address these issues. However, creating HR-HQ datasets presents two key challenges: annotation costs and reliability. Laboratory studies offer reliable annotations by using high-resolution screens and controlling viewing conditions, but they are limited in scale due to the substantial time commitment required from participants. Crowdsourcing studies are more affordable and scalable but suffer from reduced reliability caused by participants' uncontrolled viewing environments and lower-resolution displays. Consequently, creating large-scale and reliable IQA datasets for high-resolution images is an ongoing challenge.

1.3 Proposed approach

We propose an approach to creating a reliable NR-IQA database for training machine learning models. Our method addresses the limitations of existing datasets by focusing on three key aspects. First, we enhance the reliability of crowdsourcing through an improved user interface that controls display conditions across different screens. Second, we introduce reliability controls without needing ground truth by leveraging the participants' long-term self-consistency. Third, we engage expert participants to ensure annotation quality. We source CC0-licensed stock photos from Pixabay.com, to curate a dataset of high-quality images. However, because a large portion (∼40%) of the top-ranked images were not authentic but computer-generated or heavily edited, we filtered them out, ensuring our dataset consists of genuine, high-quality photographs.Fig. 1 shows sample images from our dataset. This approach seeks to overcome the limitations of existing datasets and provide a valuable resource for advancing NR-IQA research and development.

2 Related Works

We will review the current IQA datasets and quality prediction models, focusing on the research opportunities created by our new dataset.

2.1 IQA Datasets

The traditional approach to IQA dataset creation was to collect a set of pristine images and subject them to (mixtures of) *artificial distortions* at multiple distortion levels, as presented in `LIVE` [18], `TID2013` [15], `CID` [8] and `KADID-10k` [11]. Training machine learning models thereon can lead to overfitting on specific degradation types and thus poor generalization, especially to *authentically distorted* images. The latter exhibit a complex composition of practically occurring distortions, such as those found in online photography platforms and social media. Consequently, research has focused on quality annotated collections of images sampled directly from practical applications.

The class of *authentically distorted* datasets consequently thrived. `LIVE in the Wild` [4] promoted both the *authentic* distortion paradigm as well as *crowdsourcing* as a viable alternative to traditional subjective annotation studies in a controlled laboratory setting. With deep neural networks in mind, `KonIQ-10k` [5] was the first larger dataset containing a wide diversity of content for model training. The sampling of this dataset aimed to ensure the selected images had a uniform distribution along multiple quality-related indicators.

Although existing IQA datasets resemble contemporary images in many respects, their annotated data does not align well with the advancements in modern camera technology, such as improvements in technical quality and resolution, as shown in Fig. 2. Image resolution has a measurable effect on perceived quality, as shown in the study presented alongside the `KonX` [23] cross-resolution IQA

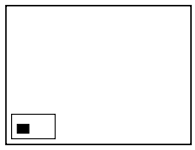

Fig. 2: Resolution discrepancy of a 1024×768px/0.7MP image (filled rectangle) as used in many IQA datasets vs. a 3840×2160px UHD/8.3MP image (inner frame) that is common in our new dataset. The outer frame illustrates a 16320×12240px/200MP image captured by recent smartphone sensors, pointing to future challenges.

dataset. In short, down-scaling has the largest effect on medium-quality images, improving their appearance. This is less the case for the high and low end of the quality scale; thus, excellent and poor quality images are generally unaffected by scaling and stay at their respective level of subjective quality. Furthermore, the authors [23] highlight the importance of the reliability of subjective ratings. They argue that consistency in repeated ratings helps reduce the noise in individual annotations. The noise can arise from participants' variable degree of attention, random saliency effects, or biases and misinterpreting the scale. Participants who give similar ratings on a second presentation of an image are likely to have lower overall noise. Thus, self-consistency checks are essential. Nevertheless, the annotation and presentation methods in IQA are still evolving with just noticeable differences as a relatively new approach investigating finely nuanced differences [3].

As indicated in Fig. Fig. 2, the curse of dimensionality presents a significant challenge in assessing high-resolution images. The increased sparsity of higher dimensions might need more annotated data, straining computational resources and limiting the generalization of IQA methods. Researchers have developed datasets that link global image quality with local patch-based assessments to address this. The concept of patch-wise quality was introduced in `KonPatch-30k` [22] and expanded in `Paq-2-Piq` [24]. In addition, distortion-strength labeled datasets like `KADIS-700k` [11] enhance the generalization of IQA models via self-supervision [2, 13]. These datasets might lead to new methods that work well on high-resolution images.

Among existing datasets, the most similar to ours is the `HRIQ` [6] dataset. It comprises 1120 images with a size of 2880×2160px annotated in a lab study, with participants primarily recruited from university students. The proposed dataset improves over `HRIQ` in the number of images and their resolution. Moreover, our annotators were all selected from photographers/graphics professionals who work with high-resolution screens in their conventional environments. This led to more reliable labels than regular crowd workers or lab studies.

We report a comparison between existing IQA datasets in Tab. 1.

Table 1: Comparison between existing IQA datasets.

Database	Source Images	Distortion Types	Distortion Levels	Distorted Images	Annotation Strategy	Image Resolution	Year
LIVE [18]	29	5		799	lab study	mostly 768 × 512px	2006
TID2008 [16]	25	17	4	1700	remote + lab	512 × 384px	2008
CSIQ [8]	30	6	4 or 5	866	lab study	512 × 512px	2010
TID2013 [15]	25	24	5	3000	remote + lab	512 × 384px	2013
CID2013 [20]	480	(12-14 cameras)	–	–	lab study	variable / 1600 × 1200px	2013
KADID-10k [11]	81	25	5	10125	crowdsourcing	512 × 384px	2019
KonIQ-10k [5]	10073	–	–	–	crowdsourcing	1024 × 768px	2018
PaQ-2-PiQ [24]	39810	–	–	–	crowdsourcing	variable	2020
KonX [23]	420	–	–	–	freelancers	max 2048 × 1536px	2023
HRIQ [6]	1120	–	–	–	lab study	2880 × 2160px	2024
UHD-IQA (Ours)	6073	–	–	–	freelancers	mostly 3840 × 2160px	2024

2.2 Auxiliary Image Datasets

Beyond IQA, several other image databases [10, 12, 14, 25] might help create predictive models. For instance, one way to do this is to pre-train an image encoder in a self-supervised manner [1, 2, 13].

Alternatively, one could employ datasets annotated for related tasks. An example is the `AVA` [14] datasets, which underscores image aesthetics rather than their technical quality. Nonetheless, the two tasks are different, and training on aesthetics-related labels could only be marginally beneficial for predicting technical quality.

Image restoration datasets [10, 12, 25] might also be suited for pre-training. For instance, `LSDIR` is a large-scale dataset for image restoration comprising about 87,000 high-resolution images collected from Flickr. These images were manually inspected by human annotators to ensure high quality. Zhang *et al.* [25] introduce the `UHDSR4K` and the `UHDSR8K`, which contain 8099 images of 4K resolution and 2966 images of 8K resolution. The images in these datasets are collected from the Internet and depict a broad range of content.

2.3 NR-IQA Models

In recent years, No-Reference Image Quality Assessment has drawn significant interest and has been studied in several works [1,2,9,13,19,21,23], given its practical applications in both research and industry settings. Supervised learning has proved to be an effective technique for NR-IQA, as demonstrated by the performance of several methods relying on it [9, 19, 23]. For instance, HyperIQA [19] introduces a self-adaptive hypernetwork that separates content understanding from quality prediction. The model is trained on 224×224 image patches by minimizing the L_1 loss between the predicted and ground truth quality scores.

A different line of research is based on pre-training a self-supervised image encoder and then learning a linear regression using the labeled MOS [2, 13]. For example, ARNIQA [2] pre-trains the encoder by maximizing the similarity between different images degraded by a similar procedure. Hence, the encoder

learns to generate similar representations for images with similar distortion patterns, regardless of their content.

Recently, several works [1,21,26] have tackled NR-IQA by relying on vision-language models, such as CLIP [17]. CLIP-IQA [21] employs an out-of-the-box CLIP model to compute the quality score by measuring the similarity between the image and two antonym prompts, such as "Good/Bad photo". CLIP-IQA+ [21] additionally learns the antonym prompts using the labeled MOS. In contrast, QualiCLIP [1] improves over CLIP-IQA by employing a self-supervised quality-aware image-text alignment strategy to make CLIP generate representations that correlate with the intrinsic quality of the images.

Despite the large variety of approaches and techniques presented above, none of these methods are designed for high-resolution images. As a result, it is challenging to fully utilize the detailed information available in UHD images. We hope that the release of our dataset will foster research on approaches specifically tailored for handling high-resolution images effectively and efficiently.

3 Database Sampling

The images composing our dataset were sampled from Pixabay[4]. We indexed an initial collection of images classified as photos, amounting to about 150,000 images of resolutions greater than UHD-1 (3840×2160px). These were sorted by normalized favorites [23], and the top 10,000 were selected for further sampling. Among these, a subjective study was conducted to remove synthetic images. Participants were instructed to identify all synthetic images, such as those that appear to be computer-generated renderings or drawings, and pay special attention to those that are difficult to distinguish from real photographs but are likely not authentic.

(a) Graphic renderings **(b)** Photo composites **(c)** Overly edited

Fig. 3: Examples of synthetic images removed from the initial collection, leaving only authentic photos in the annotated dataset. The authors of the images are, from left to right: 'ColiN00B', 'stokpic', and 'jplenio' from Pixabay.com.

For photo composites, participants should exclude images that contain elements that cannot exist in real life. Additionally, they should identify images

[4] https://pixabay.com

that have been overly or badly edited, where the edits result in unrealistic or implausible visuals, such as extreme color adjustments or exposure enhancements. We show examples of images removed from the initial collection in Fig. 3. The remaining 6,073 images constitute our proposed dataset.

4 Subjective Study

To collect an IQA database, we conducted a subjective study using the IQAvi web application [23]. Participants were presented with a series of images and asked to rate their quality on a scale from "bad" (1%) to "excellent" (100%).

4.1 Experimental Setup

Participants were required to use the Chrome browser on a display with a diagonal larger than 14 inches and a native resolution greater than 2560×1440px. The browser was set to full-screen mode during the experiment, and participants were instructed to adjust their screen brightness and contrast to clearly see image details. A fast internet connection (5+ Mbps) was recommended to minimize image-loading delays. Before the main experiment, participants completed a training session to familiarize themselves with the quality rating scale and the types of image defects to consider. The training session included images with gold-standard quality ratings to help participants calibrate and anchor their judgments. The ground-truth images and ratings were sourced from 2048×1536 pixel images from the KonX database [23].

During the main experiment, participants were presented with sequences of images and used a slider to assign a quality rating to each image. They were instructed to thoroughly explore each image for visible defects by panning as needed. Participants were also informed that high resolution does not always imply high quality and that they should focus on the level of degradation independent of the display resolution.

4.2 Quality Assessment Criteria

Participants were instructed to assess the technical quality of images based on the level of *annoyance caused by visible defects*, such as noise, blur, compression artifacts, and color distortions. They were informed that technical quality is distinct from aesthetic appeal or attractiveness and that images with high technical quality are not always highly aesthetically pleasant. However, participants were also advised that in certain cases, such as macro or close-up photography, some defects, such as background blur ("bokeh"), may be an intrinsic part of the composition and should only be considered as quality-degrading when they become annoying to the observer.

4.3 Participant Selection

To ensure the subjective study's quality and reliability, a rigorous participant selection was employed. Freelancers with backgrounds in graphics design and photography were invited to participate in the experiment. Some of these individuals had prior experience with quality assessment through their work in photo processing, printing, or as published photographers. The selection process involved an initial training phase followed by test rounds, where images with known ground-truth quality scores were presented to the participants. The ground-truth quality scores were based on the Mean Opinion Scores (MOS) of images from the `KonX` database, with an acceptable range of $\pm$ 1 standard deviation. Participants' responses were considered correct if they fell within these predefined intervals. Of the 25 initial contestants, 15 met the accuracy and correlation requirements during the test phase. These requirements included an accuracy greater than 60% and a Spearman's Rank Correlation Coefficient (SRCC) greater than 0.75 relative to the ground-truth MOS.

However, two participants were later removed from the final dataset due to an incomplete submission and another three due to unreliable performance during the main study. This resulted in 10 reliable participants whose responses were used for the analysis. The stringent participant selection process, which included training, testing, and ongoing performance monitoring, aimed to ensure that the collected subjective quality scores were consistent, reliable, and representative of the perceived image quality.

4.4 Annotation Procedure and Reliability Measures

The annotation was conducted in two rounds, each involving the same set of images. To ensure unbiased assessments, images were presented in randomized batches - the same images were presented in a different order each time. The order of the batches was also randomized for each participant. Furthermore, each batch was presented several days apart to mitigate potential biases. This was achieved by ensuring that a batch was repeated only after the participant had seen at least half of the other batches between presentations.

Measures of Reliability We compared the Mean Opinion Scores (MOS) from the first and second rounds to assess the experiment's reliability or repeatability. This comparison yielded a Spearman's Rank Correlation Coefficient (SRCC) of 0.93 and a Root Mean Square Error (RMSE) of 0.03 on the test set, indicating a high consistency between the two annotations rounds.

Another measure of reliability or repeatability of the experiment was the agreement between groups of participants. We sampled equal-sized non-overlapping groups of participants and compared their MOS. The group's size went up to 5 from a total of 10. This group-wise MOS comparison provides a lower bound for the overall reliability of 10 vs. 10 participants, which is our primary interest. The results, illustrated in Fig. 4, indicate an expected SRCC of at least 0.87 and an RMSE of at most 0.055 for the 10 vs. 10 participant comparison.

Implications for Model Performance The comparisons between virtual groups of 10 vs. 10 participant agreement and the first vs. second round MOS offer insights into the expected performance of predictive models. While models have the potential to "denoise" the original ratings and thereby achieve higher performance relative to the noisy ground truth, their success depends on their generalization capabilities. However, as we will see in the next section, baseline models have not yet reached the precision observed in the MOS derived from groups of 5 participants.

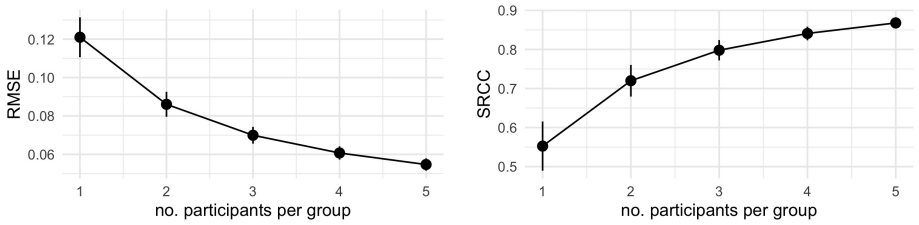

Fig. 4: (a): RMSE between MOS of groups on the test set. (b): SRCC between MOS of groups on the test set. The error bars are ± standard deviation of the performance metrics.

5 Discussion

5.1 Analysis

Our dataset comprises 6073 labeled examples, all of which were resized to a fixed width of 3840 pixels. The height was proportionally scaled to maintain the original's aspect ratio. Thus, some images are shorter than the standard 2160 pixels.

We split the dataset into about 70%, 15%, and 15% for the training, validation, and test sets, respectively. We report the exact number of examples for each split in Fig. 5a. Starting from the test split, we employ a stratified sampling strategy to achieve a distribution of the MOS that is as close as possible to a uniform one [23]. Consequently, as shown in Fig. 5b, the test and validation splits contain a wider range of labeled MOS than the training one. This creates a more challenging scenario for the models, as they must generalize to unseen image quality scores to perform well on our dataset. Thus, we argue that models achieving high performance on our dataset will likely be suitable for contemporary high-quality and resolution images.

5.2 Model performance evaluation

We investigate the performance of several state-of-the-art NR-IQA methods on our dataset. To provide a comprehensive analysis, we consider models based on

Split	# of examples
Training	4269
Validation	904
Test	900
Total	6073

(a)

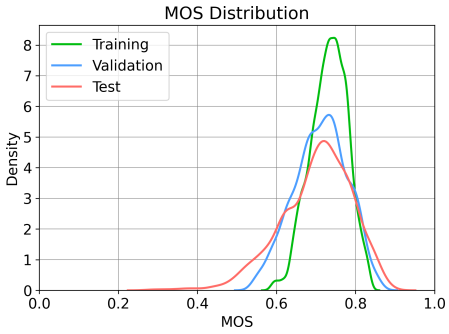

(b)

Fig. 5: (a): number of examples constituting each dataset split. (b): distribution of the labeled MOS of each dataset split.

a broad range of approaches, such as standard supervised learning [19, 23], self-supervised learning [2,13], and vision & language [1,21]. For a fair comparison, we train each model on the training split of our dataset using the hyperparameters specified by the authors in the respective paper. In particular, for methods based on self-supervised learning and vision & language, we keep the encoder weights frozen and learn a linear regressor and the prompts [21], respectively.

We employ multiple metrics for performance evaluation, namely Kendall's Rank Correlation Coefficient (KRCC), Pearson's Linear Correlation Coefficient (PLCC), Spearman's Rank-order Correlation Coefficient (SRCC), Root Mean Squared Error (RMSE), and Mean Absolute Error (MAE). We do not apply logistic regression to the predictions before computing PLCC, as the model fitting results are hard to reproduce across different works [7]. Additionally, we assess the computational efficiency of the models by measuring the number of Multiply-Accumulations operations (MACs) required for a forward pass with an input image size of 3840×2160 pixel.

We report the results on the validation and test set in Tab. 2 and Tab. 3, respectively. First, we observe that HyperIQA [19] achieves significantly lower performance than the other baselines. We attribute this outcome to the fact that HyperIQA computes the final quality score as the average of 25 different 224×224 random patches extracted from the input image. In contrast, the other methods take the whole image as input and output a single quality score. Even though the strategy adopted by HyperIQA leads to considerably fewer MACs, it does not take full advantage of the amount of information contained in high-resolution images. Second, we notice that CLIP-based models, namely CLIP-IQA+ [21] and QualiCLIP [1], obtain the best results according to the correlation-based metrics (KRCC, PLCC, and SRCC) metrics but fall behind when considering the error-based ones (RMSE and MAE). We suppose this is because CLIP-IQA+ and QualiCLIP compute the quality score based on the cosine similarity between the input image and two antonym prompts. Due to the way CLIP is trained [17], this cosine similarity can span the entire $[0, 1]$ range. Therefore, the predicted

quality scores cover a broader range than the one of the ground-truth MOS (see Fig. 5b), leading to higher absolute errors. Finally, we observe that the self-supervised learning baselines (*i.e.* CONTRIQUE [13] and ARNIQA [2]) achieve the most balanced performance, as they obtain good results for all the metrics while requiring fewer MACs than CLIP-based models.

We are only considering performance in a broad sense. We have not studied the generality of the baseline models outside the scope of the database and its inherent biases. For instance, we have not analyzed model fairness relative to the different characteristics of the images and the subjects depicted. The preferences towards certain image types of the Pixabay.com community determine inherent biases that can exist in the trained models. This could lead to spurious correlations between the types of subjects and quality levels.

Table 2: Evaluation of the performance of the baselines on the validation set. ↑ means that higher values are better, ↓ means that lower values are better. Best and second-best scores are highlighted in bold and underlined, respectively.

Method	KRCC ↑	PLCC ↑	RMSE ↓	MAE ↓	SRCC ↑	MACs (G) ↓
HyperIQA [19]	0.359	0.182	0.087	0.055	0.524	**211**
Effnet-2C-MLSP [23]	0.445	0.627	0.060	0.050	0.615	<u>345</u>
CONTRIQUE [13]	0.521	0.712	**0.049**	**0.038**	0.716	855
ARNIQA [2]	0.523	0.717	<u>0.050</u>	<u>0.039</u>	0.718	855
CLIP-IQA+ [21]	<u>0.546</u>	<u>0.732</u>	0.108	0.087	<u>0.743</u>	895
QualiCLIP [1]	**0.557**	**0.752**	0.079	0.064	**0.757**	901

Table 3: Evaluation of the performance of the baselines on the test set. ↑ means that higher values are better, ↓ means that lower values are better. Best and second-best scores are highlighted in bold and underlined, respectively.

Method	KRCC ↑	PLCC ↑	RMSE ↓	MAE ↓	SRCC ↑	MACs (G) ↓
HyperIQA [19]	0.389	0.103	0.118	0.070	0.553	**211**
Effnet-2C-MLSP [23]	0.491	0.641	<u>0.074</u>	<u>0.059</u>	0.675	<u>345</u>
CONTRIQUE [13]	0.532	0.678	**0.073**	**0.052**	0.732	855
ARNIQA [2]	0.544	0.694	<u>0.074</u>	**0.052**	0.739	855
CLIP-IQA+ [21]	<u>0.551</u>	<u>0.709</u>	0.111	0.089	<u>0.747</u>	895
QualiCLIP [1]	**0.570**	**0.725**	0.083	0.066	**0.770**	901

6 Conclusion

We introduced a novel NR-IQA dataset that offers several significant advantages. First, it is the largest UHD and highest-quality IQA database available. Second, it features annotations at higher resolutions than existing IQA datasets for training NR-IQA models. Third, it offers a unique opportunity to evaluate the performance of IQA methods in challenging and practical conditions. Our dataset offers a way forward for model development, extending observations from previous works regarding cross-resolution generalization [23] and high-resolution IQA [6]. Including perceptual quality ratings from expert raters and rich metadata ensures it is comprehensive and reliable for training. Current computer vision methods are increasingly required to perform efficiently and accurately at high resolutions. We believe NR-IQA should also tackle this challenge, which will significantly advance the field and foster the development of practical NR-IQA models that apply to modern, high-quality photos.

Acknowledgements

The dataset creation was funded by the Deutsche Forschungsgemeinschaft (DFG, German Research Foundation) – Project-ID 251654672 – TRR 161.

References

1. Agnolucci, L., Galteri, L., Bertini, M.: Quality-aware image-text alignment for real-world image quality assessment. arXiv preprint arXiv:2403.11176 (2024)
2. Agnolucci, L., Galteri, L., Bertini, M., Del Bimbo, A.: ARNIQA: Learning Distortion Manifold for Image Quality Assessment. In: Proceedings of the IEEE/CVF Winter Conference on Applications of Computer Vision. pp. 189–198 (2024)
3. Chen, G., Lin, H., Wiedemann, O., Saupe, D.: Localization of just noticeable difference for image compression. In: 2023 15th International Conference on Quality of Multimedia Experience (QoMEX). pp. 61–66. IEEE (2023)
4. Ghadiyaram, D., Bovik, A.C.: Massive online crowdsourced study of subjective and objective picture quality. IEEE Transactions on Image Processing **25**(1), 372–387 (2015)
5. Hosu, V., Lin, H., Sziranyi, T., Saupe, D.: Koniq-10k: An ecologically valid database for deep learning of blind image quality assessment. IEEE Transactions on Image Processing **29**, 4041–4056 (2020)
6. Huang, H., Wan, Q., Korhonen, J.: High resolution image quality database. In: ICASSP 2024 - 2024 IEEE International Conference on Acoustics, Speech and Signal Processing (ICASSP). pp. 3105–3109 (2024). https://doi.org/10.1109/ICASSP48485.2024.10446520
7. Kastryulin, S., Zakirov, J., Prokopenko, D., Dylov, D.V.: Pytorch image quality: metrics for image quality assessment. arXiv preprint arXiv:2208.14818 (2022)
8. Larson, E.C., Chandler, D.M.: Most apparent distortion: full-reference image quality assessment and the role of strategy. Journal of electronic imaging **19**(1), 011006–011006 (2010)

9. Li, D., Jiang, T., Jiang, M.: Norm-in-norm loss with faster convergence and better performance for image quality assessment. In: Proceedings of the 28th ACM International conference on multimedia. pp. 789–797 (2020)
10. Li, Y., Zhang, K., Liang, J., Cao, J., Liu, C., Gong, R., Zhang, Y., Tang, H., Liu, Y., Demandolx, D., Ranjan, R., Timofte, R., Van Gool, L.: LSDIR: A Large Scale Dataset for Image Restoration. In: 2023 IEEE/CVF Conference on Computer Vision and Pattern Recognition Workshops (CVPRW). pp. 1775–1787. IEEE, Vancouver, BC, Canada (Jun 2023). https://doi.org/10.1109/CVPRW59228.2023.00178
11. Lin, H., Hosu, V., Saupe, D.: Kadid-10k: A large-scale artificially distorted iqa database. In: International Conference on Quality of Multimedia Experience (QoMEX). pp. 1–3. IEEE (2019)
12. Liu, J., Liu, D., Yang, W., Xia, S., Zhang, X., Dai, Y.: A comprehensive benchmark for single image compression artifact reduction. IEEE Transactions on image processing **29**, 7845–7860 (2020)
13. Madhusudana, P.C., Birkbeck, N., Wang, Y., Adsumilli, B., Bovik, A.C.: Image quality assessment using contrastive learning. IEEE Transactions on Image Processing **31**, 4149–4161 (2022)
14. Murray, N., Marchesotti, L., Perronnin, F.: Ava: A large-scale database for aesthetic visual analysis. In: 2012 IEEE conference on computer vision and pattern recognition. pp. 2408–2415. IEEE (2012)
15. Ponomarenko, N., Jin, L., Ieremeiev, O., Lukin, V., Egiazarian, K., Astola, J., Vozel, B., Chehdi, K., Carli, M., Battisti, F., et al.: Image database tid2013: Peculiarities, results and perspectives. Signal Processing: Image Communication **30**, 57–77 (2015)
16. Ponomarenko, N., Lukin, V., Zelensky, A., Egiazarian, K., Carli, M., Battisti, F.: Tid2008: A database for evaluation of full-reference visual quality assessment metrics. Advances of modern radioelectronics **10**(4), 30–45 (2009)
17. Radford, A., Kim, J.W., Hallacy, C., Ramesh, A., Goh, G., Agarwal, S., Sastry, G., Askell, A., Mishkin, P., Clark, J., et al.: Learning transferable visual models from natural language supervision. In: International conference on machine learning. pp. 8748–8763. PMLR (2021)
18. Sheikh, H.R., Wang, Z., Cormack, L., Bovik, A.C.: Live image quality assessment database release 2. http://live.ece.utexas.edu/research/quality (2005)
19. Su, S., Yan, Q., Zhu, Y., Zhang, C., Ge, X., Sun, J., Zhang, Y.: Blindly assess image quality in the wild guided by a self-adaptive hyper network. In: Proceedings of the IEEE/CVF Conference on Computer Vision and Pattern Recognition. pp. 3667–3676 (2020)
20. Virtanen, T., Nuutinen, M., Vaahteranoksa, M., Oittinen, P., Häkkinen, J.: CID2013: A database for evaluating no-reference image quality assessment algorithms **24**(1), 390–402. https://doi.org/10.1109/TIP.2014.2378061, conference Name: IEEE Transactions on Image Processing
21. Wang, J., Chan, K.C., Loy, C.C.: Exploring clip for assessing the look and feel of images. In: Proceedings of the AAAI Conference on Artificial Intelligence. vol. 37, pp. 2555–2563 (2023)
22. Wiedemann, O., Hosu, V., Lin, H., Saupe, D.: Disregarding the big picture: Towards local image quality assessment. In: 2018 Tenth international conference on quality of multimedia experience (QoMEX). pp. 1–6. IEEE (2018)
23. Wiedemann, O., Hosu, V., Su, S., Saupe, D.: Konx: Cross-resolution image quality assessment. Quality and User Experience **8**(1), 8 (Dec 2023). https://doi.org/10.1007/s41233-023-00061-8

24. Ying, Z., Niu, H., Gupta, P., Mahajan, D., Ghadiyaram, D., Bovik, A.: From patches to pictures (paq-2-piq): Mapping the perceptual space of picture quality. In: Proceedings of the IEEE/CVF Conference on Computer Vision and Pattern Recognition. pp. 3575–3585 (2020)
25. Zhang, K., Li, D., Luo, W., Ren, W., Stenger, B., Liu, W., Li, H., Yang, M.H.: Benchmarking ultra-high-definition image super-resolution. In: Proceedings of the IEEE/CVF international conference on computer vision. pp. 14769–14778 (2021)
26. Zhang, W., Zhai, G., Wei, Y., Yang, X., Ma, K.: Blind image quality assessment via vision-language correspondence: A multitask learning perspective. In: Proceedings of the IEEE/CVF conference on computer vision and pattern recognition. pp. 14071–14081 (2023)